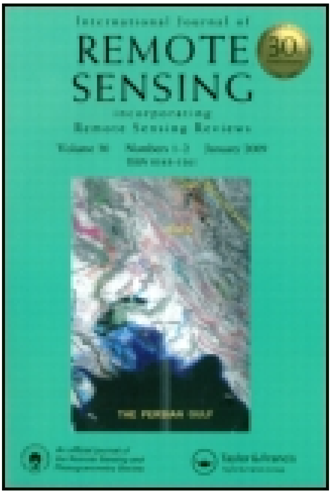

International Journal of Remote Sensing
Publication details, including instructions for authors and subscription information:
http://www.tandfonline.com/loi/tres20

Study of crop growth parameters using Airborne Imaging Spectrometer data

N. K. Patel , C. Patnaik , S. Dutta , A. M. Shekh & A. J. Dave

Published online: 25 Nov 2010.

INT. J. REMOTE SENSING, 2001, VOL. 22, NO. 12, 2401–2411

Study of crop growth parameters using Airborne Imaging Spectrometer data

N. K. PATEL, C. PATNAIK, S. DUTTA

Agricultural Resources Group, Space Applications Centre (ISRO), Ahmedabad 380 015, India

A. M. SHEKH and A. J. DAVE

Gujarat Agricultural University, Anand 388 110, India

(*Received 7 December 1998; in final form 11 April 2000*)

Abstract. High-spectral-resolution data of the Airborne Imaging Spectrometer (AIS) developed by the Indian Space Research Organisation were analysed to check their potential for extraction of information concerning crop growth parameters. Reflectance spectra of wheat plots at different growth stages were generated to study the position of red edge. The shift of inflection wavelength towards longer wavelength was observed with increase in Leaf Area Index (LAI) and chlorophyll content. For the range of LAI from 0.08 to 3.16 and chlorophyll content from 2 to 39 (gm^{-2}), the shift of inflection wavelength was observed in the range of 713–723 nm. A linear relationship was observed between the inflection wavelength and LAI as well as chlorophyll content.

1. Introduction

The imaging spectrometer provides reflectance spectra through a sequence of contiguous bands. These data have a capability to detect sharp absorption features manifested due to composition and certain physical, chemical and biophysical condition of materials (Rast 1991). Within the optical region of the electromagnetic spectrum, natural surfaces and plants are characterized through absorption features due to water, chlorophyll and minerals. The most dominating factor for study of vegetation is chlorophyll content, which causes spectral distortion. The studies have been concentrated on the transition of the reflectance between the red and near-infrared regions of the spectrum. In this domain the reflectance presents a sharp increase between 670 and 760 nm, which is called 'red edge'. This red edge presents an inflection point, the wavelength of which depends on the plant status (Collins 1978, Baret *et al.* 1987). Guyot *et al.* (1992) has shown that the red edge has an inflection point associated with a particular wavelength specific to each plant spectra dependent on phenology and health status. Green leaves with high chlorophyll concentration show this inflection point wavelength progressively shifting towards longer wavelengths in progression to increase in Leaf Area Index (LAI). The position of the red edge is largely influenced by LAI. It is independent of soil background and solar zenith angle, and the atmosphere has a minor effect (Clevers and Buker 1991).

The potential of imaging spectrometer data for various thematic applications is summarized by Srivastava *et al.* (1998). In vegetation studies, the red edge of the

International Journal of Remote Sensing
ISSN 0143-1161 print/ISSN 1366-5901 online © 2001 Taylor & Francis Ltd
http://www.tandf.co.uk/journals

reflectance spectrum and especially the wavelength position of the red edge have been investigated in detail. A large number of studies have been carried out with field spectrometers (Boochs *et al.* 1990, Miller *et al.* 1991, Plummer *et al.* 1991). Their results show that the position and shape of the red edge contain information about the biomass, chlorophyll content and physiological stress of vegetation. Collins (1978) showed that the wavelength position of the red edge is a good parameter to describe the growth of vegetation. Clevers and Buker (1991) modelled that the inflection wavelength is strongly influenced by the LAI. Results of the study conducted during Multi-sensor Airborne Campaign (MAC) Europe '91 have shown a strong correlation between the wavelength position of the red edge and the vegetation height as well as biomass of corn (Bach *et al.* 1995). In a recent study conducted on wheat crop, Singh *et al.* (1997) detected the temporal shift of the red edge using IRS-P3 Modular Opto-electronic Sensor (MOS)-B data. The expected relation between the growth and development of wheat and the red edge of the wheat spectra may be analysed by correlations between the red edge parameters and the vegetation growth parameters.

In order to investigate the potential applications of high-spectral-resolution remote sensing data for assessment of crop growth condition, a study was conducted using data acquired during a test flight of the Airborne Imaging Spectrometer (AIS) developed by the Indian Space Research Organisation (ISRO). The main objective of this study was to check whether this type of data is capable of detecting variation in crop growth parameters such as LAI, chlorophyll content and biomass. An attempt was made to study the position of the red edge for wheat crop at different growth conditions and derive a relationship between crop growth parameters and inflection wavelength computed from red-edge parameters.

2. Study area

A wheat-growing area of Dholka Taluka (administrative block) of the Ahmedabad district, Gujarat state, was selected for this study. It is an area irrigated by the Fatehwadi canal. Sowing and harvesting of wheat crop is done in the middle of October and the middle of March, respectively. An area of approximately 10×2 km was selected for the AIS flight. The location of the study area is shown in figure 1. Four runs of flight in a north-to-south direction were planned. A reconnaissance survey was conducted before the flight. Selection of the study area was done using a false colour composite (FCC) generated by merging IRS 1C LISS III and panchromatic data. Wheat plots having different growth conditions were selected for detailed study of crop growth parameters.

3. Data used

High-spectral-resolution data were acquired on 24 and 26 February 1997 between 1100 and 1130 hrs from 3 km flight height using the AIS. The broad specifications of the AIS (Anon. 1993) are given in table 1. Ground data collection was carried out synchronous to the AIS flight. Plots were identified using the cadastral map of Visalpur village. A portable Ground Truth Radiometer (GTR) developed by the Space Applications Centre of the Indian Space Research Organisation (ISRO) was used to collect spectral data of selected plots (figure 2). The field of view of radiometer was 15° and the central wavelengths of 11 bands were 490, 565, 660, 670, 710, 745, 785, 880, 960 and 1025 nm. The bandwidth of each band was 10 nm. Measurement of reflected radiance was made holding the radiometer vertically approximately 1.5 m above a plot, and measurement of irradiance was made using barium sulphate coated

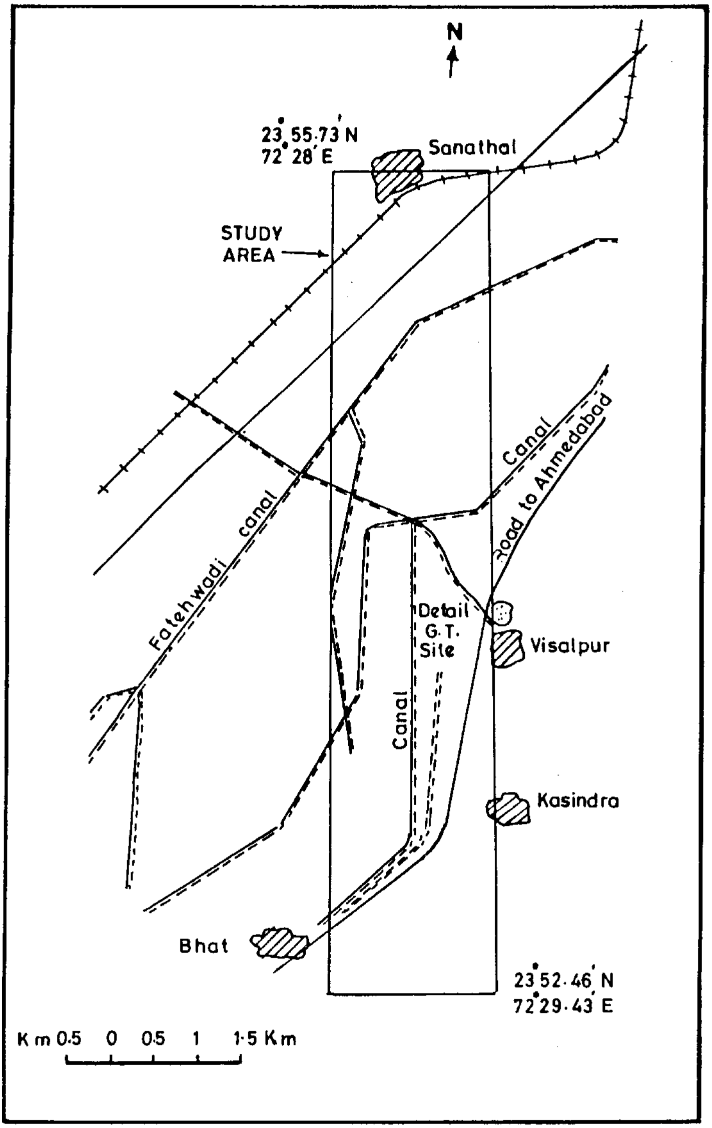

Figure 1. Location of the test site.

reference plate. Percent reflectance in each band was calculated by taking ratio of radiance to irradiance. For measurements of LAI, chlorophyll content and biomass, samples of 10 randomly selected plants were removed from each plot. Fresh weight of these plants was taken and the number of plants per $1m^2$ was counted at three places within each plot to find out the plant population. Leaf area was measured using leaf area metre LI COR model LI 3000. Computation of LAI and biomass was done using measurements of sample plants and plant population.

The chlorophyll content was determined by the method of Hiscox and Israelstam (1979). Fresh material (50 mg) chopped into small pieces was placed into test tubes containing 10 ml of dimethyl sulfoxide (DMSO), extra pure AR (Sisco Research Lab.). The tubes containing leaf tissues and DMSO were kept in an oven adjusted

Table 1. Salient features of the AIS.

1.	Instantaneous geometric field of view (μrad)	660, 2m × 2m from altitude of 3 km		
2.	Swath width (degrees) (no. of pixels)	14.5, 770m from 3 km (384)		
3.	Spectral range (nm)	450–880 nm		
4.	Encoding bits/pixel	10		
5.	Formatted bits/pixel	12		
6.	Band to band registration	Inherent		
		Raw	Spectral	Spatial
7.	Number of spectral bands	143	143	17*
8.	Spectral bandwidth (nm)	3	3	3 to 24
9.	Spatial resolution			
	Across track (mrad)	0.66	5.28	0.66
	Along track (mrad)	0.66	0.66	0.66
10.	Field of view (degrees)	14.5	14.5	14.5

* Within the specified interval.

Table 2. Crop growth parameters measured for selected fields.

Plot no.	Growth stage	Fresh biomass ($kg\,m^{-2}$)	Dry matter ($kg\,m^{-2}$)	LAI	Chlorophyll ($g\,m^{-2}$)	Plant height (cm)
W1024	Flowering	2.72	0.59	3.16	39.91	76.2
W1023	Flowering	2.14	0.56	1.75	25.77	58.3
W1020	Maturity	3.14	1.45	0.46	10.36	78.6
W1011	Flowering	1.27	0.38	0.71	13.63	68.3
W100	Maturity	0.68	0.63	0.30	2.23	56.2
W1008	Milking	2.59	1.00	1.22	16.35	83.9
W1175	Booting	1.16	0.23	1.90	15.94	43.0
W1087	Soft dough	1.23	0.53	0.83	12.55	68.3
W1165	Soft dough	3.63	1.45	1.08	27.22	83.9
W1081	Flowering	1.65	0.37	1.51	18.05	86.6
W1146	Milking	2.79	0.83	2.31	23.51	90.1
W1539	Milking	2.39	0.69	0.59	13.33	88.5
W1213	Soft dough	1.66	0.66	0.35	16.06	72.1
W1520	Flowering	0.47	0.11	0.43	5.66	51.1
W1525	Maturity	1.03	0.54	0.08	7.01	65.2
W1515	Milking	1.99	0.93	1.17	22.44	86.1
W1514	Soft dough	2.26	0.88	0.71	22.01	91.8

at 65°C temperature for about 3 h. During the incubation period, a gentle shaking was given to all the tubes. Chlorophyll was extracted into fluid, transferred to graduated tubes and made up to a total volume of 10 ml by adding extra DMSO. A 3-ml sample of chlorophyll extract was transferred to a cuvette, and absorbance was measured as the optical density values (OD) at 663 and 645 nm, using a Backman Spectrometer. Chlorophyll a, b and total chlorophyll (a + b) content (expressed as $mg\,g^{-1}$ from leaf weight) was calculated by the following equations:

$$\text{chlorophyll a} = 12.7\ E_{663} - 2.63\ E_{645} \tag{1}$$

$$\text{chlorophyll b} = 22.9\ E_{645} - 4.68\ E_{663} \tag{2}$$

$$\text{total chlorophyll} = 22.2\ E_{645} + 8.02\ E_{663} \tag{3}$$

where E_{663} and E_{645} are the absorbance values (OD) at 663 and 645 nm, respectively.

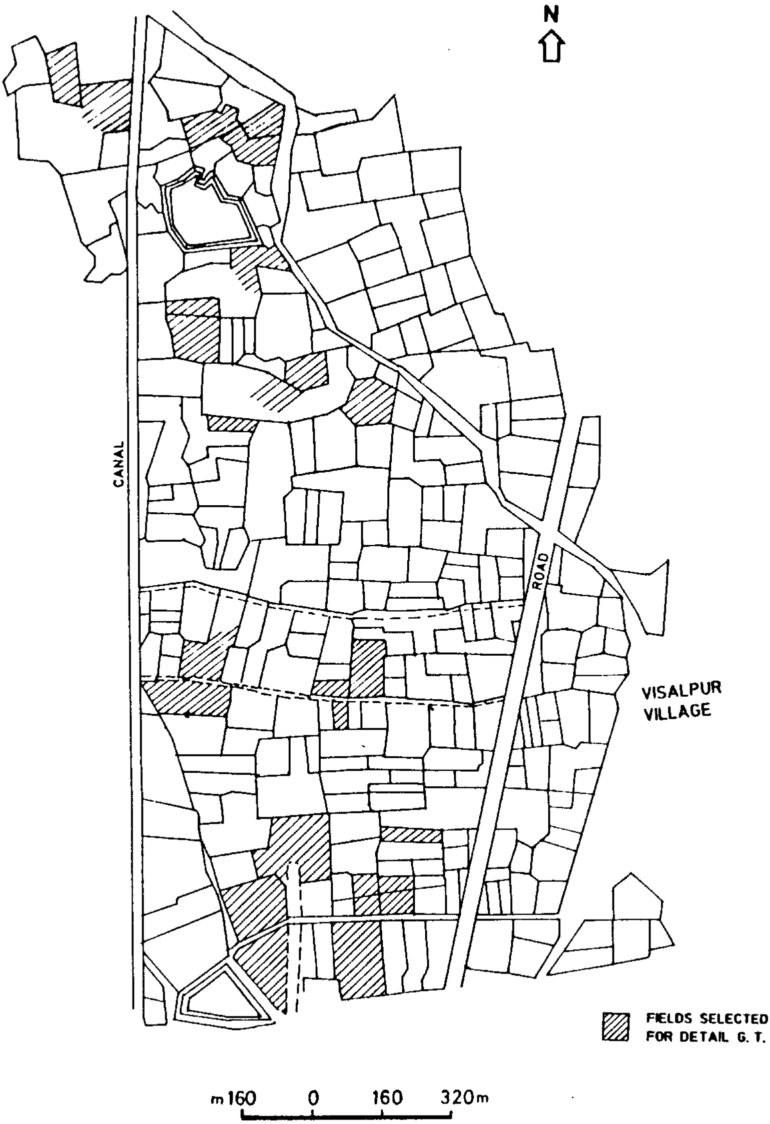

Figure 2. Location of the selected fields in Visalpur village.

4. Data analysis

The major steps involved in the data analysis are shown in figure 3. Data acquired in raw mode on 24 and 26 February 1997 were used. Data of Visalpur village were extracted and converted into a sub image of 143 bands. The FCC prepared using one each in green, red and near-infrared bands was displayed and used for identification of selected plots. Signatures of selected plots were generated in all bands and mean values of digital counts obtained. Radiometric calibration constants of gain and offset for each band provided along with the raw data were used to convert digital counts into radiance.

Wheat plots at different growth stages and bare soil (fallow plot) were selected to study spectral characteristics. Figures 4 and 5 show spectral radiance response of

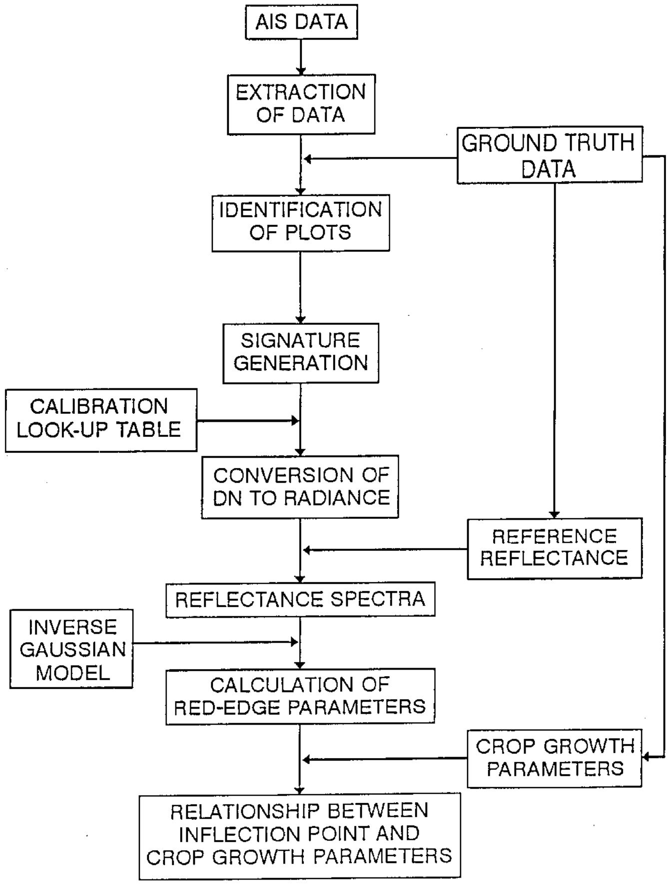

Figure 3. Major steps of the data analysis.

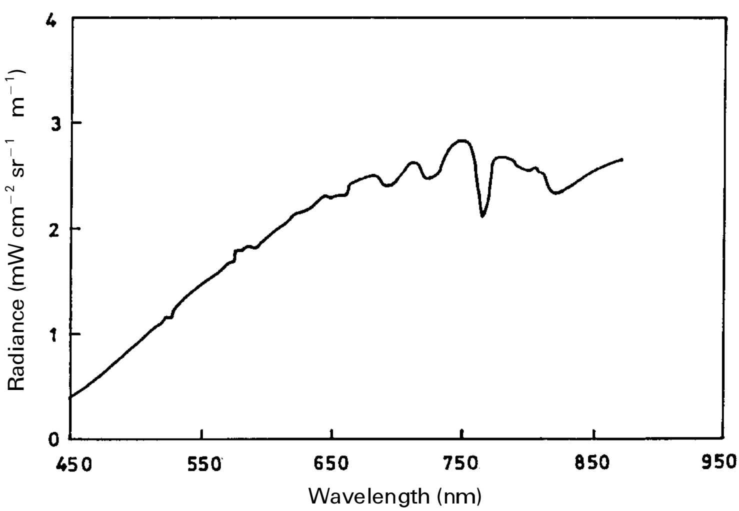

Figure 4. Spectral radiance of soil.

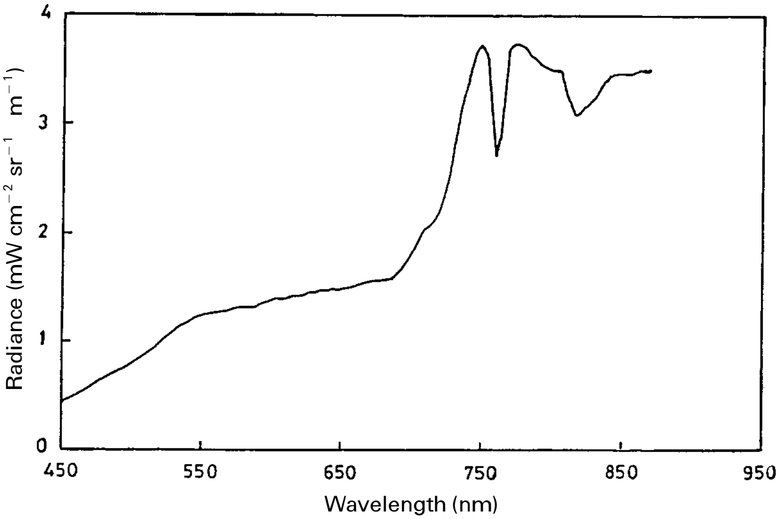

Figure 5. Spectral radiance of wheat crop.

soil and wheat, respectively. Wheat shows low radiance in the red region and higher radiance in the near-infrared region compared to soil. The absorption dip observed at 760 nm is mainly due to absorption by atmospheric oxygen (Bach *et al.* 1995). Spectral reflectance of soil (fallow plot) measured by radiometer was assumed to be same at the altitude of the AIS. Considering soil reflectance as reference, irradiance was calculated and further used to calculate percent reflectance from selected plots. Absorption by photosynthetic active biomass of crop canopy in the red region near 670 nm and high reflectance in the near-infrared region above 780 nm is observed in figure 5.

The position of the red edge is determined by inflection wavelength, which is defined as the wavelength where the rate of increase of reflectance is the maximum. The characteristics of position and shape of the red edge in the visible and near-infrared are good indicators of plant parameters. Miller *et al.* (1991) evaluated an inverted Gaussian model for the vegetation red-edge reflectance. Fitting of inverse Gaussian function to the spectral data in this region leads to four parameters, which represents the red-edge characteristics (Bach and Mauser 1991). Spectral reflectance curves for vegetation exhibit a consistent shape in the red-edge region characterized by a relatively broad flat minima in the 670 nm region, followed by a sharp increase in reflectance beginning at about 685 nm and an asymptotic reflectance plateau reached at wavelengths beyond 780 nm. The inverted Gaussian model, which represents the red edge by the reflectance, is

$$R(\lambda) = R_s - (R_s - R_0)\exp\left(\frac{-(\lambda_0 - \lambda)^2}{2\sigma^2}\right) \tag{4}$$

where R_s is the maximum or shoulder spectral reflectance, R_0 is the minimum spectral reflectance corresponding to the chlorophyll absorption well, λ_0 is the central minimum or peak absorption wavelength, λ is the wavelength in the red and near-infrared region and σ is the Gaussian function deviation parameters. A fifth parameter is λ_p, the wavelength of inflection of the red reflectance edge slope, defined by the wavelength of the maximum in the first derivative of the Gaussian function (Miller *et al.* 1990):

$$\lambda_p = \lambda_0 + \sigma \quad (5)$$

The parameter λ_p provides another measure of the position of the vegetation red reflectance edge. The standard numerical procedure is employed to produce a best fit to reflectance data according to least-square criterion. The details of the procedure are described by Bonham-Carter (1988). For inverted Gaussian model fitting, reflectance data from 650 to 780 nm were used, except data from 750 to 770 nm wavelengths due to absorption dip by atmospheric oxygen at 760 nm. This model was used for 17 plots of wheat with different growth conditions.

5. Results and discussion

The red edge is a phenomenon caused by the combination of the chlorophyll absorption in the red region and the scattering by the plant cells in the near-infrared region of the electromagnetic spectrum. The wavelength position of the red edge is known to be parameter which is sensitive to plant development (Guyot *et al.* 1992). The spectral reflectance curves of three wheat plots at different growth stages viz. flowering, soft dough and maturity stages are shown in figure 6. The difference in crop growth is reflected in spectral responses around the chlorophyll absorption in the red and near-infrared regions. Separation between spectral response of wheat plots at different growth stages increased in the region of high reflectance from 750 to 880 nm. In the near-infrared region, maximum reflectance was recorded from plot W1024, which was at the flowering stage, and more chlorophyll content and minimum reflectance was recorded from plot W1020, which was at the maturity stage. This trend was reversed at the shorter wavelengths, where the wheat plot at flowering stage exhibited enhanced absorption. Plot W1087 shows the intermediate values. This data indicate the change of reflectance values with crop growth.

The position of the red edge is determined by inflection wavelength, which is

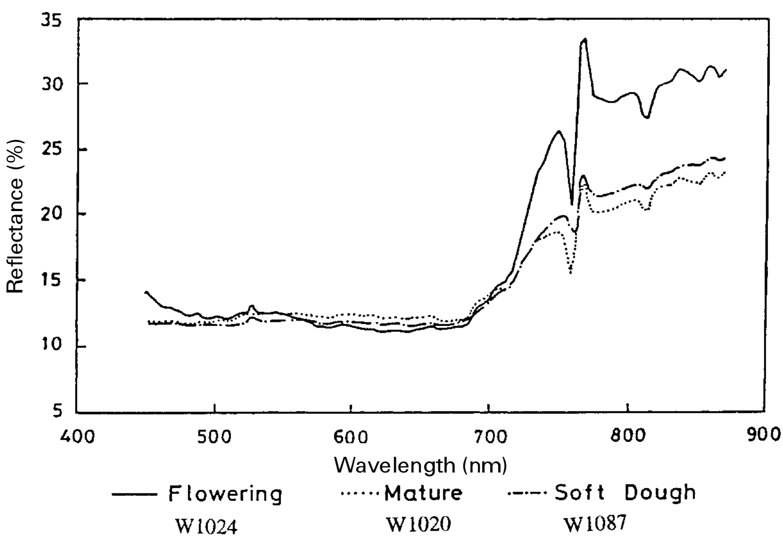

Figure 6. Spectral reflectance of wheat at different growth stages.

defined as the wavelength where the rate of increase of reflectance is the maximum. It is determined through Gaussian curve fitting to the reflectance data which can provide an effective quantitative representation of the shape and position of vegetation red-edge reflectance in terms of physical significance (Miller *et al.* 1991). The inflection wavelength of selected wheat plots was calculated using inverted Gaussian fit. Figure 7 shows the graph for three wheat plots at different LAIs. Modelling of the red edge shows longest inflection wavelength of plot number W1024, with a LAI of 3.16. The reduction in LAI and chlorophyll in the senescence phase is reflected in the graph line of plots W1087 and W1020, with LAI of 0.83 and 0.46, respectively. The shift of inflection wavelength is marked in figure 7. The chlorophyll content of plot W1024 was higher compared to the other two plots. It indicated that the position of the inflection wavelength is shifting towards longer wavelength with increase in LAI.

An attempt was made to derive a relationship between inflection wavelength and crop growth parameters. The scatter plot of inflection wavelength with LAI and chlorophyll content is shown in figures 8 and 9, respectively. Regression analysis was carried out and a linear relationship was observed between inflection wavelength and LAI and chlorophyll content. Wheat crop was in the post heading stage at the time of the AIS test flight in the month of February but, along with green leaves, dry leaves and other components, also contributed to spectral response, resulting in low values of correlation coefficients. This preliminary experiment has indicated the feasibility to study crop growth parameters using AIS data. Detailed investigation may be carried out with detailed temporal data incorporating atmospheric correction.

6. Conclusion

A shift of the inflection wavelength of spectra of wheat from 713 to 723 nm is evident for wheat plots at different growth stages. This shift was determined by extracting the inflection wavelength of the red edge of the reflectance spectra. A linear relation of inflection wavelength with LAI and chlorophyll content of wheat indicates use of high-spectral-resolution data for assessment of crop growth

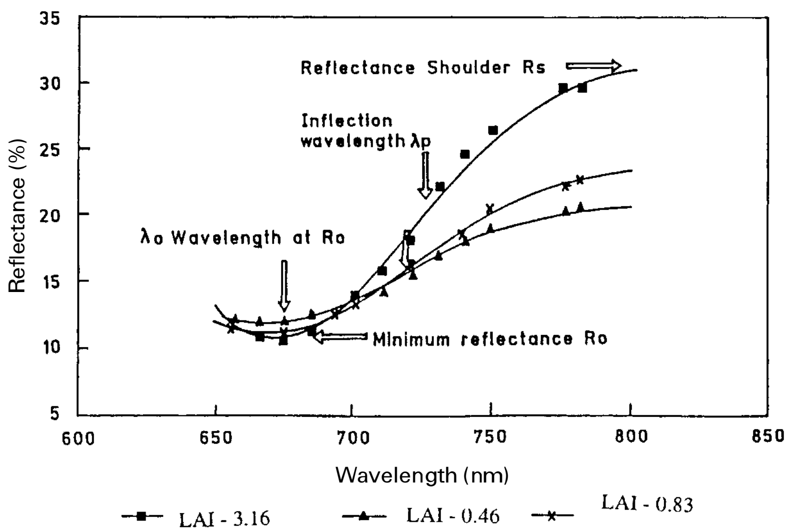

Figure 7. Inverted Gaussian fit of wheat spectra.

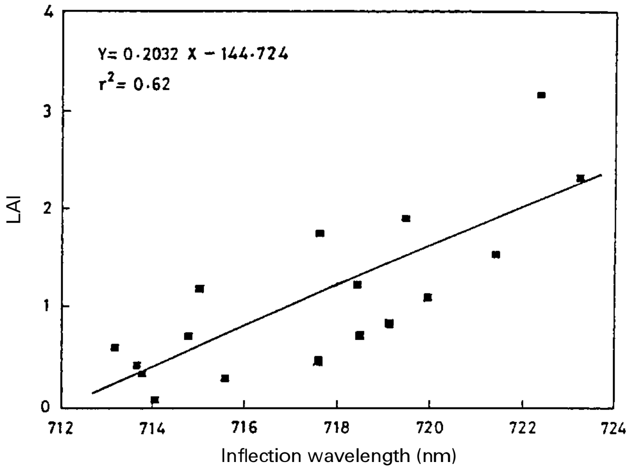

Figure 8. Relationship between inflection wavelength of wheat spectra and LAI.

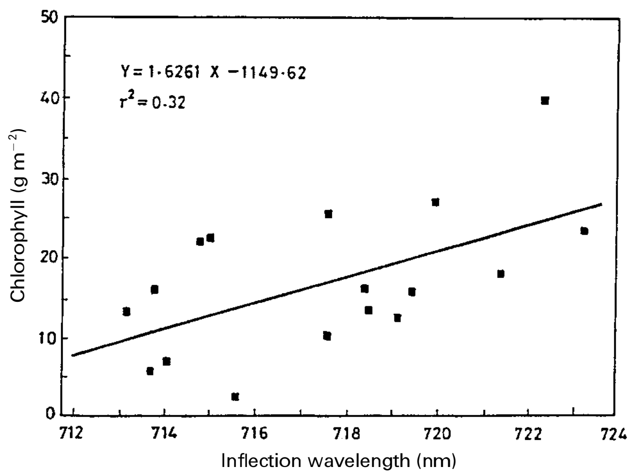

Figure 9. Relationship between inflection wavelength of wheat spectra and chlorophyll content.

conditions and identification of stressed crop. This study has provided an opportunity for understanding data acquired by an imaging spectrometer and the utility of this data in the study of crop growth parameters, and it has highlighted the need for further research into understanding the spectral response of crops grown under different growth conditions.

Acknowledgments

The authors are grateful to Dr R. R. Navalgund (Deputy Director, Remote Sensing Applications Area) and Shri J. S. Parihar (Group Director, Agricultural Resources Group) for encouragement and guidance. They are also thankful to Shri A. S. Kirankumar and Shri V. H. Patel for providing AIS data. Support provided by Shri N. P. Pandya for flight planning and software provided by Shri R. P. Singh are gratefully acknowledged.

References

Anon., 1993, Design and development of Airborne Imaging Spectrometer. SAC/EOSDG/AIS/09/93, Space Applications Centre, Ahmedabad, India.

Bach, H., Demircan, A., and Mauser, W., 1995, The use of AVIRIS data for the determination of agricultural plant development and water content. *Proceedings of MAC Europe '91—Final Results.* ESA WPP-88 (Paris: ESA), Lenggries, Germany.

Bach, H., and Mauser, W., 1991, Extraction of agricultural parameters from imaging spectrometry data and simulated MERIS data through red edge analyses. European Imaging Spectroscopy Aircraft Campaign. ESA SP-360 (Noordwijk: ESA).

Baret, F., Champion, I., Guyot, G., and Podaire, A., 1987, Monitoring wheat canopies with a high spectral resolution radiometer. *Remote Sensing of Environment*, **22**, 367–378.

Bonham-Carter, G. F., 1988, The numerical procedures and computer program for fitting an inverted Gaussian model to vegetation reflectance data. *Geoscience*, **14**, 339–356.

Boochs, F., Kufer, G., Docker, K., and Kuhbauch, W., 1990, Shape of the red edge as vitality indicator for plants. *International Journal of Remote Sensing*, **11**, 1741–1753.

Clevers, J. G. P. W., and Buker, C., 1991, Feasibility of the red edge index for the detection of nitrogen deficiency. *Proceedings of the Fifth International Colloquium, Physical Measurements and Signatures in Remote Sensing*, 14–18 January, Courchevel, pp. 165–168.

Collins, W., 1978, Remote Sensing of crop type and maturity. *Photogrammetric Engineering and Remote Sensing*, **44**, 43–55.

Guyot, G., Baret F., and Jacuemoud, S., 1992, Imaging spectroscopy for vegetation studies. In *Fundamentals and Prospective Applications*, edited by F. Toselli and J. Bodechtel (Kluwer Academic), pp. 145–165.

Hiscox, J. D., and Israelstam, C. F., 1979, A method for the extraction of chlorophyll from leaf tissue without maceration, Caadian. *Journal of Botany*, **57**, 1332–1334.

Miller, J. R., Hare, E. W., and Wu, J., 1990, Quantitative characterization of vegetation red edge reflectance: an inverted-Gaussian reflectance model. *International Journal of Remote Sensing*, **2**, 1755–1773.

Miller, J. R., Jiyou Wu, Boyer, M. G., Belanger, M., and Hare, E. W., 1991, Seasonal patterns in leaf reflectance red edge characteristics. *International Journal of Remote Sensing*, **12**, 1509–1523.

Plummer, S. E., Wilson, A. K., and Jones, A. K., 1991, On the relationship between high spectral resolution canopy reflectance data and plant biochemistry. *EARSeL Advances in Remote Sensing*, **1**, 27–33.

Rast, M., 1991, Imaging spectroscopy and its aplication in spaceborne systems. ESA SP-1144, December 1991.

Singh, R. P., Oza, S. R., and Dadhwal, V. K., 1997, Detection of red edge shift from temporal growth of wheat crop using high resolution imaging MOS-B spectrometer data. *NNRMS Bulletin*, **B-21**, 49–53.

Srivastava, S. K., Nageswara, Rao, P. P., and Jayaraman, V., 1998, Towards space-borne terrestrial imaging spectrometry. ISRO-NNRMS-SR-41-98, Indian Space Research Organisation, Bangalore.